JACS
JOURNAL OF THE AMERICAN CHEMICAL SOCIETY
Communication
pubs.acs.org/JACS

Downstream Oligonucleotides Strongly Enhance the Affinity of GMP to RNA Primer–Template Complexes

Chun Pong Tam,[†,‡,Δ] Albert C. Fahrenbach,[†,§,Δ] Anders Björkbom,[†,∥] Noam Prywes,[†,‡] Enver Cagri Izgu,[†] and Jack W. Szostak*[,†,§,‡]

[†]Howard Hughes Medical Institute, Department of Molecular Biology and Center for Computational and Integrative Biology, Massachusetts General Hospital, 185 Cambridge Street, Boston, Massachusetts 02114, United States

[‡]Department of Chemistry and Chemical Biology, Harvard University, 12 Oxford Street, Cambridge, Massachusetts 02138, United States

[§]Earth Life Science Institute, Tokyo Institute of Technology, 2-12-1-IE-1 Ookayama, Meguro-ku, Tokyo, 152-8550, Japan

[∥]Department of Biosciences, Åbo Akademi University, Åbo FI-20520, Finland

Supporting Information

ABSTRACT: Origins of life hypotheses often invoke a transitional phase of nonenzymatic template-directed RNA replication prior to the emergence of ribozyme-catalyzed copying of genetic information. Here, using NMR and ITC, we interrogate the binding affinity of guanosine 5′-monophosphate (GMP) for primer–template complexes when either another GMP, or a helper oligonucleotide, can bind downstream. Binding of GMP to a primer–template complex cannot be significantly enhanced by the possibility of downstream monomer binding, because the affinity of the downstream monomer is weaker than that of the first monomer. Strikingly, GMP binding affinity can be enhanced by ca. 2 orders of magnitude when a helper oligonucleotide is stably bound downstream of the monomer binding site. We compare these thermodynamic parameters to those previously reported for T7 RNA polymerase-mediated replication to help address questions of binding affinity in related nonenzymatic processes.

Originally proposed by Crick[1] and Orgel[2] in 1968, the nonenzymatic template-directed replication of RNA is an essential aspect of what has come to be known[3] as the RNA world hypothesis.[4−7] This model suggests that RNA, or perhaps a similar nucleic acid,[8] played a dual role, serving as both a genetic and catalytic polymer.[9−11] Chemically driven RNA replication, which permits the earliest transmission of genetic information from parent protocells to their progeny, arguably forms the foundation for the Darwinian evolution of catalytic RNA sequences, or ribozymes, that could aid in genome replication and protocell metabolism.

Although nonenzymatic template-directed RNA polymerization with activated monomers has been studied since the 1960s,[6,12−14] basic thermodynamic aspects remain unclear. The proposed mechanisms[15] start with a reversible noncovalent binding event in which the activated monomer associates with the template. These interactions can be aided by base stacking from either upstream[16−20] or downstream[19,21−24] adjacent mono- or oligonucleotides. A common experimental protocol employs a template that is annealed to a shorter primer, which can then be extended by making use of activated monomers such as 5′-phosphoro-2-methylimidazolide ribonucleotides.[14] Although the primer enhances the binding of the first monomer through adjacent upstream base stacking,[18−20,25] two questions remain: (*i*) how tightly do subsequent downstream monomers bind, and (*ii*) to what degree do downstream mono- or oligonucleotides enhance the binding of upstream monomers? Richert et al. have used primer-extension inhibitor assays to assess the effect of downstream oligomers using DNA, for which binding constant enhancements of up to ∼7-fold were observed;[19] however, direct thermodynamic measurements on RNA-based systems are still needed.

Here we describe the results of our investigations into the effects of downstream elements on the association of GMP to RNA. We measure the binding constants for the Watson–Crick association of GMP to four different primer–template complexes (Figure 1): one with a single template binding site (5′-C), another with two binding sites (5′-CC), and two more with binding sites supported by both upstream and downstream oligonucleotides. Using ^{1}H NMR spectroscopy and isothermal titration calorimetry

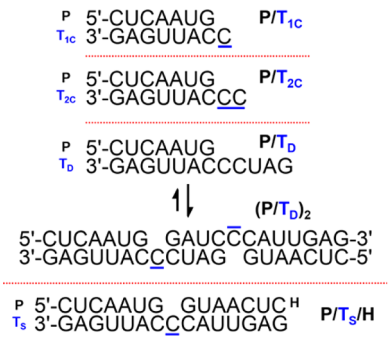

Figure 1. Sequences of the RNA duplexes studied by ITC and/or ^{1}H NMR. Each duplex contains a common seven-nucleotide primer **P** and a complementary template strand containing various binding sites for GMP (C, blue underlines). See Figures S1–S5 for detailed characterizations.

Received: September 17, 2016
Published: January 5, 2017

DOI: 10.1021/jacs.6b09760
J. Am. Chem. Soc. 2017, 139, 571−574

(ITC), we characterize the increase in affinity for GMP caused by downstream stacking elements. We demonstrate that when two GMP molecules bind in a consecutive fashion, the second monomer is more weakly bound than the first, and for this reason, a downstream monomer is unable to significantly enhance the occupancy of its neighboring upstream binding site. On the other hand, replacement of the second GMP by a stably bound downstream oligomer enhances the binding affinity of the first upstream GMP by approximately 100-fold.

We conducted NMR titrations[18] to quantify the binding of GMP to four different RNA primer−template complexes, each possessing distinct templating regions. The templates were designed to assess how different downstream elements affect the affinity of GMP. The sequences of these duplexes are displayed in Figure 1. The 7-nt primer shared by all duplexes is labeled **P**. The four different templating strands are labeled **T**, with subscripts that indicate the nature of the templating regions ($\mathbf{T}_{1C}$, $\mathbf{T}_{2C}$, $\mathbf{T}_{D}$, $\mathbf{T}_{S}$). When paired with primer **P**, templates $\mathbf{T}_{1C}$ and $\mathbf{T}_{2C}$ display one and two cytidine nucleotides on their 5′-termini, respectively. Templates $\mathbf{T}_{D}$ and $\mathbf{T}_{S}$ are designed such that stably bound downstream elements can also pair with the template to create single cytidine binding site(s) for GMP that are flanked by guanidine nucleotides.

Duplexes $\mathbf{P}/\mathbf{T}_{1C}$ and $\mathbf{P}/\mathbf{T}_{2C}$ were used to assess the thermodynamics governing the association of one and two GMP monomers, respectively. The length and sequence of these primer−template complexes were optimized such that (*i*) stable duplexes are formed under our NMR titration conditions and (*ii*) the imino proton signals are defined and well resolved[18] from one another in the 10−15 ppm region of the proton NMR spectrum. The well-resolved imino protons of these two duplexes were monitored during the titrations in order to quantify monomer binding constants. For both the titrations of $\mathbf{P}/\mathbf{T}_{1C}$ and $\mathbf{P}/\mathbf{T}_{2C}$ with GMP, the resonance frequency of the G7 imino proton—the primer nucleotide closest to the GMP binding sites—exhibits the largest upfield shift, of ∼0.35 ppm (Figure 2), likely because of ring-current effects[26,27] emanating from the purine base of the proximally bound GMP. The fact that G7 shifts the most is consistent with specific binding of GMP to the 5′-overhangs and agrees well with our previously reported results for the binding of GMP to a single-nucleotide template overhang both in solution[18] and the solid state.[28]

We next formulated a model to measure the binding constants for $\mathbf{P}/\mathbf{T}_{2C}$ with GMP employing the sequential binding processes illustrated in Scheme 1, which is described by four microscopic equilibrium constants. See Scheme S2 of the Supporting Information (SI) for a detailed derivation procedure. We made two assumptions: (*i*) sequential binding from the 3′- to the 5′-end of the overhang is the dominant pathway (i.e., $K_x \gg K_w$), because G7 affords stacking interactions that increase monomer binding at the adjacent position at least 10-fold;[17] and (*ii*) binding of the second GMP to the 5′-terminal overhang nucleotide of $\mathbf{P}/\mathbf{T}_{2C}$ does not cause the G7 imino proton resonance to undergo additional upfield shifts, because the ring current arising from the nucleobase of the more distant second monomer is too weak to have any significant effect. With these assumptions, the binding constants for the first (K_x) and second (K_y) monomer associations were determined to be 45(3) and 16(5) M^{-1}, respectively. For comparison, the binding constant determined for the $\mathbf{P}/\mathbf{T}_{1C}$ duplex using a single-binding-site model is 72(2) M^{-1}. With respect to assumption (*ii*), we tested alternative scenarios in which the influence of the second monomer on the G7 chemical shift was nonzero; all these scenarios lead to the same

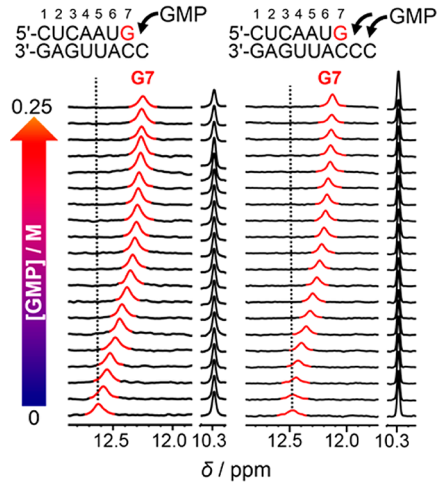

Figure 2. Stacked partial ^{1}H NMR spectra for the titrations of the $\mathbf{P}/\mathbf{T}_{1C}$ (left) and $\mathbf{P}/\mathbf{T}_{2C}$ duplexes (right) with GMP. The G7 imino proton signals are displayed. Both titrations were carried out in 10% D_2O, at 12 °C and pH 7 with 500 mM of Na^+ from 0 to 250 mM of GMP. The assignments of the imino protons for both duplexes were carried out by a combination of ^{1}H−^{1}H 2D NOESY and variable temperature ^{1}H NMR spectroscopy (Figures S2−S4). Figure S6 shows the stacked spectra of both GMP−$\mathbf{P}/\mathbf{T}_{1C}$ and GMP−$\mathbf{P}/\mathbf{T}_{2C}$ titrations, showing the complete imino proton region (10−15 ppm) with the signals of all of the other imino protons. The change in chemical shift of all seven imino proton resonances plotted against the concentration of GMP is shown in the SI (Figure S7 for $\mathbf{P}/\mathbf{T}_{1C}$, Figure S8 for $\mathbf{P}/\mathbf{T}_{2C}$). Circular dichroism spectroscopy was performed on these two duplexes, and both display spectral characteristics indicative of canonical A-form conformation (Figure S14).

Scheme 1. Proposed GMP Binding Mechanism for the $\mathbf{P}/\mathbf{T}_{2C}$ Duplex[a]

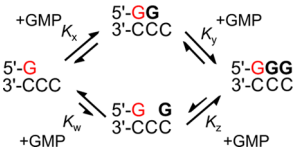

[a]Only the nucleotides constituting the binding sites for GMP are shown. For more details see SI, Scheme S2.

conclusion that K_x is larger than K_y. The values of K_x range between 40(1) and 68(2) M^{-1}, and K_y ranges between 14(2) and 42(1) M^{-1} (Figure S12), respectively. For a detailed discussion of how these alternative scenarios of second monomer binding influence the G7 shift, see Section 5 of the SI. We propose that the weaker binding of the second monomer is a consequence of the greater conformational freedom of the bound upstream monomer resulting in a less preorganized stacking surface in comparison to that of G7 in the primer.

We now turn to the question of the degree to which downstream oligonucleotides can enhance the binding of upstream monomers. To study this in depth, we designed the palindromic $(\mathbf{P}/\mathbf{T}_{D})_2$ duplex (Figure 1), in which the $\mathbf{T}_{D}$ strand possesses a 5′-overhang that consists of a cytidine residue for GMP binding, followed by a self-complementary CUAG region that allows for dimerization of the duplex. The C_2 symmetry of the dimerized duplex allows straightforward assignment of all observed imino signals. The $(\mathbf{P}/\mathbf{T}_{D})_2$ duplex contains two identical binding pockets that are supported by both upstream and downstream oligonucleotides, allowing us to determine the

DOI: 10.1021/jacs.6b09760
J. Am. Chem. Soc. 2017, 139, 571−574

degree to which a stably bound downstream element enhances the association of GMP.

The ^{1}H NMR titration of $(\mathbf{P}/\mathbf{T_D})_2$ with GMP (Figures S9 and S10) revealed that the association is in the tight-binding regime. To accurately quantify the thermodynamic parameters of binding, we used ITC. Since the two binding pockets of the $(\mathbf{P}/\mathbf{T_D})_2$ palindromic dimer are identical, we fit the data shown in Figure 3a

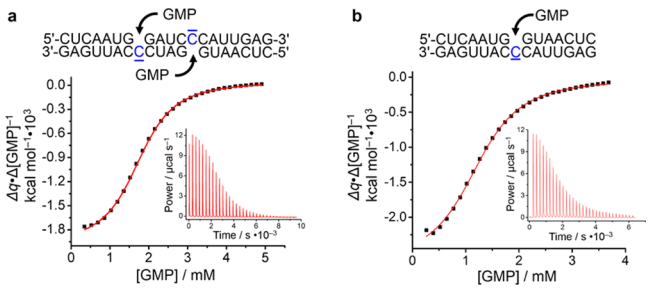

Figure 3. ITC for (a) $(\mathbf{P}/\mathbf{T_D})_2$ and (b) $\mathbf{P}/\mathbf{T_S}/\mathbf{H}$. Conditions: $(\mathbf{P}/\mathbf{T_D})_2$: 2 mM duplex in both the cell and syringe, with additional 20 mM GMP in the syringe, 12 °C; $\mathbf{P}/\mathbf{T_S}/\mathbf{H}$: 1.5 mM duplex in both the cell and syringe, with additional 15 mM GMP in the syringe, 20 °C. **Both**: 500 mM NaCl, pH 7. The red lines are the best fits from the statistical-binding isotherm derived in Section 4b of the SI for (a) and a single-binding-site isotherm for (b). Insets: raw power versus time curves. The circular dichroism spectra of both duplexes display spectral characteristics that are indicative of canonical A-form duplexes (Figure S14).

to a two-site model that assumes statistical binding[29] (see SI for the derivation, Scheme S1). The observed binding constant, K_{OBS}, was $7.3(3) \times 10^3$ M^{-1} ($\Delta G_{OBS}(12\ °C) = -5.04(2)$ kcal mol^{-1}), which is approximately 100-fold greater than the binding constant for $\mathbf{P}/\mathbf{T_{1C}}$, and potentially over 150-fold greater than the first binding constant (K_x) for $\mathbf{P}/\mathbf{T_{2C}}$. For detailed thermodynamic parameters for the GMP−$(\mathbf{P}/\mathbf{T_D})_2$ association, see Table 1. The

Table 1. Summary of Thermodynamic Parameters[a]

Duplex	K, M^{-1}	ΔG, kcal mol^{-1}	ΔH, kcal mol^{-1}	ΔS, cal mol^{-1} K^{-1}
$\mathbf{P}/\mathbf{T_{1C}}$[b]	72(2)	−2.42(2)	–	–
$\mathbf{P}/\mathbf{T_{2C}}$[b]	K_x: 45(3)	−2.16(4)	–	–
	K_y: 16(5)	−1.6(2)		
$(\mathbf{P}/\mathbf{T_D})_2$[c]	$7.3(3) \times 10^3$	−5.04(2)	−12.1(1)	−24.8(4)
$\mathbf{P}/\mathbf{T_S}/\mathbf{H}$[d]	$6.1(4) \times 10^3$	−5.08(4)	−15.7(3)	−36(1)

[a]All values determined at pH 7 and 500 mM NaCl. [b]Determined by NMR at 12 °C. [c]Determined by ITC at 12 °C. [d]Determined by ITC at 20 °C. Values shown in parentheses are errors for the last significant digit determined from the fits.

stoichiometric factor n was found to be 1.84, which is consistent with a 2:1 complex. Note that the possible incomplete dimerization or alternative secondary structures of $(\mathbf{P}/\mathbf{T_D})_2$ at the beginning of the titration will lead to a lower effective concentration of $(\mathbf{P}/\mathbf{T_D})_2$ under our experimental conditions. Hence, our experimentally obtained K_{OBS} may represent the lower limit of the true value, and the actual binding constant K may be significantly larger than that observed here.[30]

In order to provide insight into the possibility that incomplete dimerization of $\mathbf{P}/\mathbf{T_D}$ attenuates the observed binding constant, we designed the "sandwich" duplex $\mathbf{P}/\mathbf{T_S}/\mathbf{H}$ that possesses a much more stably bound downstream helper oligonucleotide **H** (see Figure S11 for the NMR titration). ITC carried out on this duplex at 20 °C (Figure 3b) revealed a similar binding constant for GMP of $6.1(4) \times 10^3$ M^{-1} and a stochiometric factor n of 0.88. See Table 1 for a summary of the thermodynamics for all duplexes. This rather large binding constant is consistent with a simple nearest-neighbor analysis,[31] which predicts a binding constant on the order of 10^4 M^{-1} (see Section S8, SI). A previously reported DNA-based sandwich complex,[19] which in a similar fashion flanks an incoming dGMP monomer by two dG nucleotides, leaves the binding constant nearly unchanged compared to when the downstream oligomer is absent. We propose the A-form helical structure of RNA leads to better base-stacking than B-form DNA, resulting in the ∼100-fold increase in affinity.

The experiments described herein constitute a quantitative basis for understanding observations associated with non-enzymatic replication. For example, Richert and co-workers[19,21,22,24] observed that helper oligonucleotides that bind downstream of activated monomers moderately improve the rate of primer extension. We also observed an increase in rate when carrying out primer extension reactions comparing $(\mathbf{P}/\mathbf{T_D})_2$ (0.11(1) h^{-1}) to $\mathbf{P}/\mathbf{T_{1C}}$ (0.039(1) h^{-1}) (Figure S13). At least part of this ∼3-fold rate enhancement can be explained by tighter binding of guanosine 5′-phosphoro-2-methylimidazolide, a thermodynamic effect that increases the fraction of the reactive monomer-bound complex. Using the binding constants measured herein to take this effect into account, we estimate the downstream oligomer only contributes catalytically a factor of ∼2-fold to this increase in observed rate.

Some other aspects of primer extension reactions, however, cannot be explained by the same thermodynamic effects. For example, Orgel and co-workers have demonstrated that the rate of nonenzymatic primer extension with respect to the first addition is increased by the presence of downstream templating sites, especially when monomers activated with 2-methylimidazole are employed; the rate of addition is on the order of 20 times faster.[32] We observe a similar increase in rate when comparing $\mathbf{P}/\mathbf{T_{2C}}$ (0.42(1) h^{-1}) to $\mathbf{P}/\mathbf{T_{1C}}$ (0.039(1) h^{-1}), the former of which is nearly 10 times faster under our conditions (Figure S13). Using the binding constants measured herein, we calculate that that binding site occupancies for $\mathbf{P}/\mathbf{T_{1C}}$ and the first position of $\mathbf{P}/\mathbf{T_{2C}}$ are comparable (∼70−80%). Therefore, the thermodynamics of sequential monomer binding cannot account for the rate-enhancing effect previously hypothesized to be caused by a neighboring downstream activated monomer.[23] We recently reported that the mechanistic origin of this kinetic effect, at least in some cases, is likely a result of the prior formation of an imidazolium-bridged dinucleotide intermediate, which binds more tightly to the template, is more reactive, or both.[33] Whether or not such an intermediate might itself be synthesized on the template, or formed only transiently as part of a concerted mechanism, is still under investigation.

Finally, how do the thermodynamic parameters described herein compare to those measured for an enzymatically assisted primer-extension reaction, e.g., one involving the T7 RNA polymerase? Such a comparison offers an important empirical way to evaluate upper bounds for binding parameters that could lead to acceptable levels of fidelity and rate in the nonenzymatic primer-extension reactions. In essence, such a side-by-side juxtaposition allows us to address the question, how tight is tight enough? The T7 RNA polymerase employs an allosteric mechanism,[34−36] switching from an "open" state, in which the complementary nucleotide triphosphate (NTP) can base-pair to the N+1 site of the DNA template, to a catalytically active "closed" state. It is informative to note that the affinities of NTP substrates to the T7 RNA polymerase ternary complex (measured as K_m

DOI: 10.1021/jacs.6b09760
J. Am. Chem. Soc. 2017, 139, 571−574

constants during elongation of 76−190 *u*M or K_{assoc} (5.3−13) × 10^3 M^{-1})[37] are on par with the binding constants measured here for GMP association with $(\mathbf{P}/\mathbf{T_D})_2$ or $\mathbf{P}/\mathbf{T_S}/\mathbf{H}$, although alternative sandwich complexes employing pyrimidine stacking surfaces may result in much less enhancement. With this caveat in mind, downstream helper oligomers can potentially offer sufficient enhancement of monomer binding, and seeking even tighter binding of activated monomers is not necessary. On the other hand, when comparing the effective rate constant for enzymatic replication (taking into account initiation, elongation and termination), the T7 RNA polymerase is about 10^6 times faster[38] than what we observe for $\mathbf{P}/\mathbf{T_{2C}}$ (115 s^{-1} vs 0.4 h^{-1}). The challenge in nonenzymatic replication, at least from the perspective of this comparison, is not so much thermodynamic as it is kinetic. With respect to fidelity, the allosteric mechanism of the enzymatic reaction acts to "amplify" the selectivity of Watson−Crick pairing, as only correctly paired NTPs are able to favor the switch to the closed state,[39] thereby helping to ensure high-accuracy copying.

The thermodynamic studies that we have performed point to the fact that the two different mechanisms by which a downstream oligomer or an activated monomer increase the rate of extension are complementary to each other. We recently demonstrated in a separate report that the rates of nonenzymatic template-directed synthesis indeed can be further improved by employing *activated* helper oligomers.[23] Using this approach, the rate constant increases up to about 1 min^{-1} and an average fidelity of 98% can be achieved, which is sufficiently high to enable the copying of ∼50 nt-long mixed-sequence templates, the length of some functional RNAs. Additional investigations into the exact mechanistic effect(s) responsible for the observed fidelity, including a means for selectivity "amplification", are underway. Understanding the cooperative self-assembly and primer-extension kinetics of activated monomer and downstream oligonucleotides with a wide range of RNA sequences will bring the origins of life community significantly closer to achieving rapid and high-fidelity nonenzymatic copying of catalytically active RNA.

■ ASSOCIATED CONTENT

Supporting Information

The Supporting Information is available free of charge on the ACS Publications website at DOI: 10.1021/jacs.6b09760.

Methods, Schemes S1−S2, and Figures S1−S14 (PDF)

■ AUTHOR INFORMATION

Corresponding Author

*szostak@molbio.mgh.harvard.edu

ORCID

Chun Pong Tam: 0000-0001-6381-9011

Enver Cagri Izgu: 0000-0001-6673-3635

Author Contributions

[Δ]C.P.T. and A.C.F. contributed equally.

Notes

The authors declare no competing financial interest.

■ ACKNOWLEDGMENTS

J.W.S. is an Investigator of the Howard Hughes Medical Institute. This work was supported in part by a grant from the Simons Foundation to J.W.S. (290363). A.C.F. is supported by a Research Fellowship from the Earth-Life Science Institute at the Tokyo Institute of Technology. A.B. was supported by a grant from the Academy of Finland. We thank Dr. Victor Lelyveld, Dr. Seung Soo Oh, Dr. Li Li, Dr. Aaron Engelhart, Dr. Christian Hentrich, Dr. Lijun Zhou, and the rest of the Szostak lab for helpful discussions.

■ REFERENCES

(1) Crick, F. H. C. *J. Mol. Biol.* **1968**, *38*, 367.
(2) Orgel, L. E. *J. Mol. Biol.* **1968**, *38*, 381.
(3) Gilbert, W. *Nature* **1986**, *319*, 618.
(4) Patel, B. H.; Percivalle, C.; Ritson, D. J.; Duffy, C. D.; Sutherland, J. D. *Nat. Chem.* **2015**, *7*, 301.
(5) Orgel, L. E. *Crit. Rev. Biochem. Mol. Biol.* **2004**, *39*, 99.
(6) Blain, J. C.; Szostak, J. W. *Annu. Rev. Biochem.* **2014**, *83*, 615.
(7) Adamala, K.; Szostak, J. W. *Science* **2013**, *342*, 1098.
(8) Taylor, A. I.; Pinheiro, V. B.; Smola, M. J.; Morgunov, A. S.; Peak-Chew, S.; Cozens, C.; Weeks, K. M.; Herdewijn, P.; Holliger, P. *Nature* **2015**, *518*, 427.
(9) Szczepanski, J. T.; Joyce, G. F. *Nature* **2014**, *515*, 440.
(10) Johnston, W. K.; Unrau, P. J.; Lawrence, M. S.; Glasner, M. E.; Bartel, D. P. *Science* **2001**, *292*, 1319.
(11) Bartel, D. P.; Doudna, J. A.; Usman, N.; Szostak, J. W. *Mol. Cell. Biol.* **1991**, *11*, 3390.
(12) Sulston, J.; Lohrmann, R.; Orgel, L. E.; Miles, H. T. *Proc. Natl. Acad. Sci. U. S. A.* **1968**, *59*, 726.
(13) Lohrmann, R.; Bridson, P. K.; Orgel, L. E. *Science* **1980**, *208*, 1464.
(14) Kozlov, I. A.; Orgel, L. E. *Mol. Biol.* **2000**, *34*, 781.
(15) Fahrenbach, A. C. *Pure Appl. Chem.* **2015**, *87*, 205.
(16) Davies, R. J. H.; Davidson, N. *Biopolymers* **1971**, *10*, 1455.
(17) Kanavarioti, A.; Hurley, T. B.; Baird, E. E. *J. Mol. Evol.* **1995**, *41*, 161.
(18) Izgu, E. C.; Fahrenbach, A. C.; Zhang, N.; Li, L.; Zhang, W.; Larsen, A. T.; Blain, J. C.; Szostak, J. W. *J. Am. Chem. Soc.* **2015**, *137*, 6373.
(19) Kervio, E.; Claasen, B.; Steiner, U. E.; Richert, C. *Nucleic Acids Res.* **2014**, *42*, 7409.
(20) Kervio, E.; Sosson, M.; Richert, C. *Nucleic Acids Res.* **2016**, *44*, 5504.
(21) Vogel, S. R.; Deck, C.; Richert, C. *Chem. Commun.* **2005**, 4922.
(22) Röthlingshöfer, M.; Kervio, E.; Lommel, T.; Plutowski, U.; Hochgesand, A.; Richert, C. *Angew. Chem., Int. Ed.* **2008**, *47*, 6065.
(23) Prywes, N.; Blain, J. C.; Del Frate, F.; Szostak, J. W. *eLife* **2016**, *5*, e17756.
(24) Hagenbuch, P.; Kervio, E.; Hochgesand, A.; Plutowski, U.; Richert, C. *Angew. Chem., Int. Ed.* **2005**, *44*, 6588.
(25) Sawada, T.; Fujita, M. *J. Am. Chem. Soc.* **2010**, *132*, 7194.
(26) Gomes, J. A. N. F.; Mallion, R. B. *Chem. Rev.* **2001**, *101*, 1349.
(27) Wannere, C. S.; Schleyer, P. v. R. *Org. Lett.* **2003**, *5*, 605.
(28) Zhang, W.; Tam, C. P.; Wang, J.; Szostak, J. W. *ACS Cent. Sci.* **2016**, *2*, 916.
(29) Connors, K. A. *Binding Constants: the Measurement of Molecular Complex Stability*; Wiley: New York, 1987.
(30) Larsen, A. T.; Fahrenbach, A. C.; Sheng, J.; Pian, J.; Szostak, J. W. *Nucleic Acids Res.* **2015**, *43*, 7675.
(31) Turner, D. H.; Sugimoto, N.; Freier, S. M. *Annu. Rev. Biophys. Biophys. Chem.* **1988**, *17*, 167.
(32) Wu, T.; Orgel, L. E. *J. Am. Chem. Soc.* **1992**, *114*, 5496.
(33) Walton, T.; Szostak, J. W. *J. Am. Chem. Soc.* **2016**, *138*, 11996.
(34) Temiakov, D.; Patlan, V.; Anikin, M.; McAllister, W. T.; Yokoyama, S.; Vassylyev, D. G. *Cell* **2004**, *116*, 381.
(35) Steitz, T. A. *Curr. Opin. Struct. Biol.* **2009**, *19*, 683.
(36) Steitz, T. A. In *RNA Polymerases as Molecular Motors*; Buc, H., Strick, T., Eds.; RSC Pub.: Cambridge, U.K., 2009; p 96.
(37) Vaught, J. D.; Dewey, T.; Eaton, B. E. *J. Am. Chem. Soc.* **2004**, *126*, 11231.
(38) Arnold, S.; Siemann, M.; Scharnweber, K.; Werner, M.; Baumann, S.; Reuss, M. *Biotechnol. Bioeng.* **2001**, *72*, 548.
(39) Sydow, J. F.; Cramer, P. *Curr. Opin. Struct. Biol.* **2009**, *19*, 732.

DOI: 10.1021/jacs.6b09760
J. Am. Chem. Soc. 2017, 139, 571−574